

High-energy Neutrinos from Neutron Star Mergers

Shigeo S. Kimura

Frontier Research Institute for Interdisciplinary Sciences, Tohoku University, Sendai 980-8578, Japan
Astronomical Institute, Tohoku University, Sendai 980-8578, Japan
E-mail: shigeo@astr.tohoku.ac.jp

ABSTRACT

We investigate prospects for coincident detection of high-energy neutrinos with gravitational waves. We consider two scenarios: One is classical short gamma-ray bursts (SGRBs) with prolonged engine activities, where the extended emission component with a duration of ~ 100 seconds emit high-energy neutrinos most efficiently. The other is the choked jet system where the prompt jet fails to penetrate the ejecta of the BNS merger. We show that such choked jet systems may be common by calculating the jet propagation in the expanding ejecta. For both scenarios, the coincident neutrino detection with gravitational waves are probable if the future detector, IceCube-Gen2, is realized, or non-detection will put meaningful constraints on the parameters.

KEY WORDS: neutrinos — gravitational waves — gamma-ray burst: general

1. Introduction

In 2017, we detected the gravitational waves (GWs) and electromagnetic counterparts from a binary neutron-star (BNS) merger event, GW 170817 (Abbott et al. 2017). The optical counterpart provides the information of host galaxies and merger ejecta (Utsumi et al. 2017), and the observations of prompt gamma-rays and broadband afterglows strongly supports BNS mergers as the progenitor of SGRBs (Mooley et al. 2018; Lamb et al. 2019).

Although high-energy gamma rays and neutrinos were not detected (Albert et al. 2017; Abdalla et al. 2017), they are expected to be produced in the jet of SGRBs (Waxman & Bahcall 1997; Kimura et al. 2017; Murase et al. 2018; Kimura et al. 2019). The protons are likely to be accelerated at the dissipation region of the SGRB jets, and the accelerated protons efficiently produce π^+ and π^0 through interactions with photons observed as GRBs. The charged pions decay to muon neutrinos and anti-muons. The anti-muons also decay to electron neutrinos, anti-muon neutrinos, and positrons. The spectra of these neutrinos depend on the parent proton spectrum, target photon density, cooling processes of the parent particles (protons/pions/muons). Also, the neutrino spectrum on Earth differs from that at the source due to the flavor mixing.

We calculate the neutrino production from BNS mergers, appropriately taking the coolings of parent particles and the flavor mixing into account. Although the luminous GRBs cannot account for the bulk of the observed astrophysical neutrinos (Aartsen et al. 2017), coincident

neutrino detection with GWs from a nearby BNS merger is possible. We examine two scenarios. First, we investigate the successful SGRBs with prolonged engine activities, and then, we discuss the choked jet system where prompt jets fail to penetrate ejectas of BNS mergers (See Kimura et al. (2017); Matsumoto & Kimura (2018); Kimura et al. (2018) for details).

2. Neutrinos from SGRBs with Prolonged Activities

In the X-ray light curves of SGRBs, some show a flat component followed by an abrupt cutoff. This component (extended emission; EE) cannot be explained by the emission from the forward shock, indicating prolonged central engine activities for hundreds of seconds (Ioka et al. 2005; Sakamoto et al. 2011). Some SGRBs have additional components that may attribute to the central engine activities, such as plateau emissions and X-ray flares. The energy fluences of these components are comparable to that of the prompt emission, and thus, the prolonged engine activities are also expected to be sources of neutrinos. We estimate the neutrino fluence from each component of a typical SGRB, and plot them in Figure 1. We find that the EEs are the most strong neutrino emitter of the four owing to its lower Lorentz factor and higher luminosity.

We discuss the prospects for detection of neutrinos from EEs coincident with GWs. Assuming that half of the SGRBs have EEs and that the BNS mergers occur at 300 Mpc where GWs from BNS mergers are detectable, we compute the neutrino detection probability coinci-

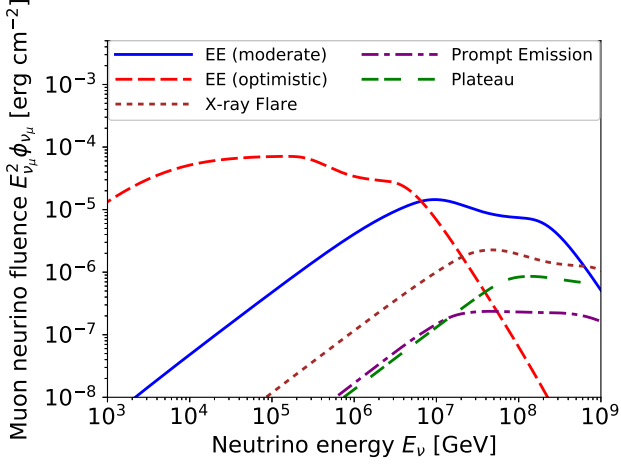


Fig. 1. Neutrino fluence from the prompt, extended, plateau, and X-ray flare components. This figure is reproduced from Kimura et al. (2017) with permission from AAS.

Table 1. Neutrino detection probability coincident with GWs with current IceCube and with future IceCube-Gen2. The top two rows are for the successful SGRB scenario with 10 years of operation. The bottom two rows are for the choked jet scenario with a year of operation. The values are taken from Kimura et al. (2017); Kimura et al. (2018)

Model	IceCube	IceCube-Gen2
EE-mod	0.11-0.35	0.37-0.77
EE-opt	0.65-0.97	0.93-1.00
Choked-mod	0.024	0.091
Choked-opt	0.38	1.2

dent with the GWs. The results are tabulated in Table 1. Here, we examine two parameter sets, optimistic (EE-opt) and moderate (EE-mod) cases, and the range of the values indicates the uncertainty of the distribution of the jet Lorentz factor. For the optimistic parameter set, the current IceCube detector likely detects a coincident neutrino, while with the moderate parameter set, we need the planned experiment, IceCube-Gen2, to expect the neutrino detection.

3. Choked Jet Systems

3.1. Jet propagation in the expanding ejecta

The observations of GW 170817 revealed that the ejecta of BNS merger is heavier than expected (Tanaka et al. 2017). Also, the prompt and afterglow emissions from GW 170817 differ from the canonical SGRBs (Kasliwal et al. 2017). To explain these, the choked jet scenario

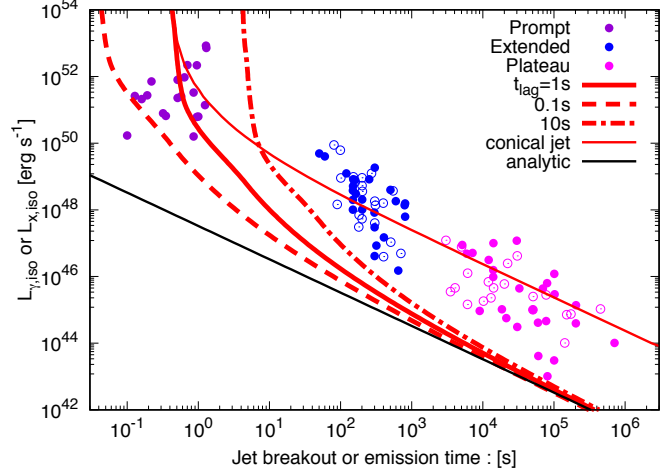


Fig. 2. Comparison of jet breakout time to the observed SGRB events. This figure is reproduced from Matsumoto & Kimura (2018) with permission from AAS.

was proposed, where the jet fails to penetrate the ejecta (Gottlieb et al. 2018). Using the quantities obtained by the optical counterpart, we calculate the propagation of the jet in the ejecta, taking the effect of ejecta expansion into account. We plot the jet breakout time as a function of the jet luminosity (thick-red lines) in Figure 2. We overplot the observed SGRB events in the figure, and find that non-negligible fraction of the prompt jets would fail to penetrate the ejecta if the time lag between ejecta production and jet launch is 1 second. This may indicate that the choked jet system is common. On the other hand, the EE and plateau components easily penetrate the ejecta because the ejecta continuously decreases its density by expansion. Hence, there can be X-ray transients or X-ray counterparts to GWs without prompt gamma-ray emissions.

3.2. Neutrinos from the choked jet system

There are three energy dissipation sites in the choked jet system. One is the jet head, where interaction between the jet and the ejecta forms shocks. The shocked matter at the jet head expands sideways and forms the cocoon surrounding the jet. The cocoon pushes the jet inward and creates the collimation shock, which is the second dissipation region in the system. The other is the internal shocks inside the pre-collimation jets, which can be formed if the central engine has a strong time variability.

Among the three dissipation sites, only the internal shocks can produce high-energy neutrinos. At the jet head, the density is so high that the shocks are mediated by radiations, where the velocity jump is gradual and non-thermal particles cannot be accelerated. In the collimation shocks and internal shocks, protons can be accelerated and produce pions if we consider moderately

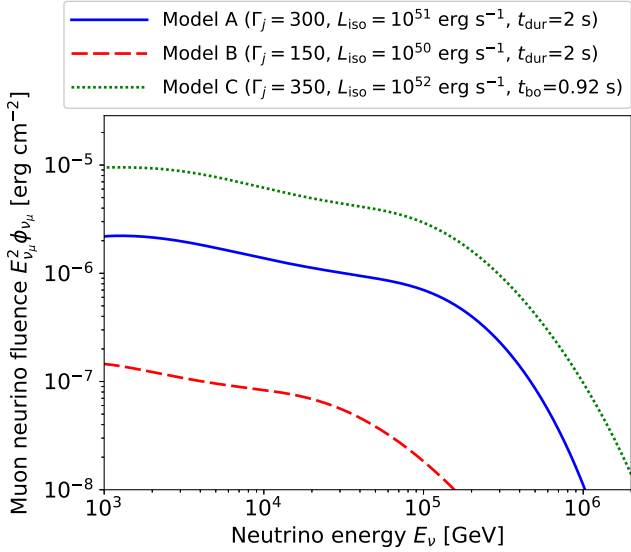


Fig. 3. Neutrino spectra from the internal shocks in the choked jet system. This figure is reproduced from Kimura et al. (2018).

high values of Lorentz factor: ~ 500 for the collimation shocks and ~ 200 for the internal shocks. At the downstream of the collimation shocks, the pions above ~ 1 TeV quickly lose their energies through synchrotron radiation or hadronic interactions, and hence, high-energy neutrinos are not produced. On the other hand, at the downstream of the internal shocks, the pions can decay to high-energy neutrinos before cooling down, since the energy density is lower there.

In the choked jet system, the target densities are extremely high owing to the compact dissipation regions, and thus, the accelerated protons completely lose their energy through the photomeson production. The neutrino spectra from the internal shocks are flat with a slight softening below the cutoff energy because of the calorimetric system and muon cooling, as shown in Figure 3. Using these spectra, we estimate the neutrino detection rate coincident with GWs, which are tabulated in Table 1. For the optimistic case (Choked-opt), we highly expect the coincident detection with a few years of operation even with IceCube. With a 10-year operation of IceCube-Gen2, the coincident detection is probable even for the moderate case (Choked-mod).

4. Summary

The multi-messenger event, GW 170817, confirmed that BNS mergers launch relativistic jets and strongly supports the BNS merger paradigm of SGRBs. Jets of SGRBs are expected to produce high-energy neutrinos through hadronic interactions. We have calculated neutrino emission from BNS mergers and discussed the fu-

ture prospects for neutrino detection coincident with GWs based on two scenarios. In the first scenario, canonical SGRBs with prolonged engine activities, the neutrinos are efficiently produced in the EEs whose duration is about 100 seconds, owing to its higher luminosity and lower Lorentz factor. As the second scenario, we discuss neutrino emission from the choked jet system where the prompt jet is blocked by the ejecta. Calculating the propagation of the jet in the ejecta, we found that considerable fraction of the observed prompt jets are unable to penetrate the ejecta of GW 170817. This implies that the choked jet system may be common. The high-energy neutrinos can be produced in the internal shocks, although other shocks in the system cannot produce them because of the high densities. For both scenarios, the high-energy neutrinos coincident with GWs can be detectable with IceCube-Gen2, and non-detection will put meaningful constraints on the physical quantities of the systems.

References

- Aartsen, M. G., Ackermann, M., Adams, J., et al. 2017, *ApJ*, 843, 112
- Abbott, B. P., Abbott, R., Abbott, T. D., et al. 2017, *ApJL*, 848, L12
- Abdalla, H., Abramowski, A., Aharonian, F., et al. 2017, *ApJL*, 850, L22
- Albert, A., André, M., Anghinolfi, M., et al. 2017, *ApJL*, 850, L35
- Gottlieb, O., Nakar, E., Piran, T., & Hotokezaka, K. 2018, *MNRAS*, 479, 588
- Ioka, K., Kobayashi, S., & Zhang, B. 2005, *ApJ*, 631, 429
- Kasliwal, M. M., Nakar, E., Singer, L. P., Kaplan, D. L., & et al. 2017, *Science*, 358, 1559
- Kimura, S. S., Murase, K., Bartos, I., et al. 2018, *PRD*, 98, 043020
- Kimura, S. S., Murase, K., Ioka, K., et al. 2019, *ApJL*, 887, L16
- Kimura, S. S., Murase, K., Mészáros, P., & Kiuchi, K. 2017, *ApJL*, 848, L4
- Lamb, G. P., Lyman, J. D., Levan, A. J., et al. 2019, *ApJL*, 870, L15
- Matsumoto, T., & Kimura, S. S. 2018, *ApJL*, 866, L16
- Mooley, K. P., Deller, A. T., Gottlieb, O., et al. 2018, *Nature*, 561, 355
- Murase, K., Toomey, M. W., Fang, K., et al. 2018, *ApJ*, 854, 60
- Sakamoto, T., Barthelmy, S. D., Baumgartner, W. H., et al. 2011, *ApJS*, 195, 2
- Tanaka, M., Utsumi, Y., Mazzali, P. A., Tominaga, N., & et al. 2017, *PASJ*, 69, 102
- Utsumi, Y., Tanaka, M., Tominaga, N., Yoshida, M., & et al. 2017, *PASJ*, 69, 101
- Waxman, E., & Bahcall, J. 1997, *PRL*, 78, 2292